Onset of flux penetration into a type-II superconductor disk

A. V. Kuznetsov and D. V. Eremenko
Department of Quantum Electronics, Moscow State Engineering Physics Institute, 115409 Moscow, Russia

V. N. Trofimov
Laboratory of Nuclear Problems, Joint Institute for Nuclear Research, 141980, Dubna, Moscow region, Russia
(Received 10 June 1996; revised manuscript received 4 February 1997)

The virgin magnetization of a type-II superconductor disk in a transverse field is discussed. The edge effects in a superconductor of rectangular cross section are considered, taking into account anisotropy and pinning. The penetration field of the geometrical barrier is calculated. It is shown that flux pinning at the edge corners influences the penetration field. The temperature dependence of the penetration field of platelike high-T_c single crystals is discussed. [S0163-1829(97)09734-8]

I. INTRODUCTION

The magnetization studies of films and single crystals of high-temperature superconductors (HTSC's) have focused attention to the problem of magnetic behavior of a thin flat superconductor in a field applied perpendicular to its plane. Significant progress has been achieved in development of the critical state model for such samples.[1–3] Within this model, virgin and remanent magnetization, flux creep, ac losses, and flux dynamics in a varying field can be calculated in the case of strong pinning.

Currently, there is a considerable interest to platelike superconductors with a weak or zero pinning. It has been found that the samples exhibit strongly hysteretic behavior,[4,5] nonuniform magnetization and domelike distribution of magnetic flux in the sample center.[6,7] Being corrected on demagnetization factor, the applied field corresponding to onset of flux penetration noticeably exceeds the lower critical field H_{c1}. This field is commonly named the penetration field H_p. The temperature dependence of H_p frequently has no saturation at low temperatures.

The above mentioned features reflect an influence of a potential barrier arising at the sample edge and preventing flux penetration. Conventional theory of the Bean-Livingston barrier[8] has been recently extended[9,10] to describe magnetization and flux creep in HTSC's. But this type of barrier is inherent to a flat superconductor when the applied field is parallel to the surface. In a transverse field the geometrical barrier[6,7,11,12] originally attributed to the rectangular cross section (in the direction along the applied field) of a sample is formed. Hysteretic magnetization and flux distribution have been described by the geometrical barrier model[7,12,13] (GBM) which gives an adequate approximation for magnetization in a field above H_p. In the present paper we discuss the magnetic behavior below or in the vicinity of H_p.

In both the critical state model and GBM a thin flat sample is approximated by a superconducting sheet. Two-dimensional distribution of normal and tangential components of field on the sheet which are proportional to flux density and sheet current, respectively, is analyzed within these models. It is quite difficult to calculate three-dimensional distribution of the field and the current for the flat sample of finite thickness d. Recently Brandt[14] has proposed a computational method for the case of strong pinning when the flux density and the critical sheet current inside a superconductor are larger then the lower critical field. Unfortunately, the extension of this method to the case of weak or zero pinning is not done yet so we cannot use it to analyze onset of flux penetration through the geometrical barrier.

In order to compute the penetration field one should treat edge effects appearing in the superconductor of rectangular cross section and calculate the field enhancement at the sample edge. In the Meissner state the field enhancement is proportional to edge curvature which is of the order of reciprocal thickness for a thin flat sample.[7,12,15] In GBM Zeldov *et al.*.[7] assumed that in increasing field the vortices initially cut through the sharp rims of a sample without complete penetration and thus effectively round off the curvature of the edge to the value of the order of $2/d$. Benkraouda and Clem[12] presented a model in which sample's edge is rounded and has a curvature radius $d/2$. The penetration field of a long strip is $H_p \simeq H_{c1}/\sqrt{a}$ within such approximations, where a is the width-to-thickness ratio of a sample named aspect ratio. That is a good estimate for a pinning-free isotropic superconductor with large aspect ratio. As a rule type-II superconductors are characterized by pinning or (and) anisotropy. Therefore in the next section we treat the case of anisotropic superconductor with pinning.

Let us consider a superconductor of rectangular cross section and thickness d in a uniform magnetic field H_a applied perpendicular to the sample plane. In the Meissner state the local field at the edge corners of the sample is strongly enhanced in comparison with applied field H_a. The local field reaches the critical value in a very weak applied field. The corners enter to the mixed state [Fig. 1(a)] but the main part of the sample remains in the Meissner state. If H_a increases, the top and the bottom mixed state regions grow until they come into the contact at the equator at $H_a = H_p$. Before that the vortices in the opposite corners are separated by the Meissner phase at the equator and penetration of magnetic flux into the center of a sample is impossible. When the field reaches H_p, flexed vortices at the equator tend to become straight due to self-line tension and migrate towards the

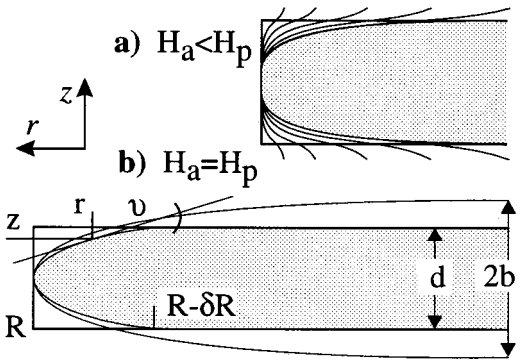

FIG. 1. Field patterns at the edge of a sample with rectangular cross section. Blank regions correspond to the mixed state, black ones to the superconducting state. Grey color in the bottom picture marks the cross section of a spheroid. The sample and the spheroid have equal diameters and curvatures at equator. For detailed explanation see the text.

sample center under influence of shielding current as it is described in GBM.

In order to evaluate H_p one should calculate a field distribution when the corners are occupied by the mixed state, as it is shown in Fig. 1. It can be done by the solution of the Laplace equation for the Meissner part of the sample with the standard boundary conditions: at infinity the field is equal to an applied one, the field is tangential at the surface of the Meissner part, and at the boundary between the Meissner and the mixed phases the field is equal to H_{c1}. The problem is the same for a type-I superconductor with the replacement of H_{c1} by H_c. Therefore one can use the results of numerical calculation of the Laplace equation performed for a cylinder of type-I superconductor[16] to treat magnetic behavior of a type-II superconductor. It was shown that (i) in a weak field the top and the bottom intermediate-state regions are separated by the Meissner-state region in the equator; (ii) the central cross section of the interphase surface represents a convex, not straight, line as one can expect for a type-I superconductor; and (iii) when the top and the bottom intermediate-state regions meet each other at the equator, the local field reaches there the critical field H_c. Using these conclusions we describe below a simple model which enables one to calculate H_p in a thin flat sample of type-II superconductor without solving the Laplace equation.

This paper is organized as follows. The model for calculation of the penetration field is considered in Sec. II. We calculate H_p dependence on aspect ratio, anisotropy and pinning. In Sec. III a comparison of the calculated and the measured penetration field is presented for HTSC's single crystals. We discuss there the temperature dependence of the penetration field taking into account pinning of vortices in the corners. We discuss also the limitations on the sample characteristics imposed by our model. Section IV contains a brief summary of our results.

II. PENETRATION FIELD OF THE GEOMETRICAL BARRIER

Let us consider a disk of anisotropic type-II superconductor with $a \gg 1$ and $d \gg \lambda$ (λ is the penetration depth) in a cylinder frame with origin in the center of the sample. A uniform field H_a is applied normally to the sample. We consider the most interesting case of an uniaxial anisotropy with the axis normal to sample plane. This case represents HTSC's when anisotropy in Cu-O planes can be neglected. In a weak field the mixed state arises in the corners. In the absence of pinning macroscopic current in the corners is equal to zero. In the presence of pinning the critical state is formed and the critical current with density J_c flows in the corners. The opposite regions of the mixed (or critical) state are separated by the Meissner-phase region and the field at the interphase surface is equal to H_{c1}. A current shielding the Meissner part of the sample flows at the interphase surface. This current is equal to a stepwise discontinuity of the tangential field at the surface, i.e., H_{c1}.

We are interested in a radial distribution of the sheet current $I(r)=Jd$, where J is the current density averaged over the sample thickness. Apart from the edge at a distance more than δR the sheet current is equal to a discontinuity of tangential field on the sample top and bottom surfaces. Here δR is the radial size of the mixed-state region at the sample face [Fig. 1(b)] called below the edge width. The sheet current I_E flowing in the rim $R<r<R-\delta R$ is equal to a sum of the critical and the Meissner currents. To obtain I_E one should calculate the angular dependence of both H_{c1} and J_c. As is known,[17,18] in an uniaxial-anisotropy superconductor the dependence of the lower critical field on the angle ϑ between field and isotropic plane may be described by the anisotropy function ε_ϑ:

$$H_{c1\vartheta}=H_{c1}\varepsilon_\vartheta\left(1-\frac{\ln\varepsilon_\vartheta}{\ln\kappa}\right), \tag{1}$$

$$\varepsilon_\vartheta=\sqrt{1-(1-\gamma)\cos^2\vartheta},$$

where H_{c1} and κ are related to isotropic plane, anisotropy parameter $\gamma=m/M$ with m and M being the effective masses in the plane and along the axis, respectively. The same function describes angular dependence of the critical current $J_{c\vartheta}=J_c\varepsilon_\vartheta$ when vortex lines have inclination angle ϑ with respect to isotropic plane.[18] J_c is also related to the plane. For the sake of simplicity we assume that the angular dependence of the critical current density averaged over the thickness of the critical-state region may be accounted for in the same way with the angle ϑ between the isotropic plane and a line tangent to the longitudinal-through-diameter cross section of interphase surface [Fig. 1(b)]. This approximation slightly lowers the critical current because at fixed r the slope of the flexed vortices and, consequently, ϑ increase from the interphase boundary to the sample's surface [Fig. 1(a)], but considerably simplifies calculations. Considering the angular dependencies, one can write

$$I_E(r)=2H_{c1}\varepsilon_\vartheta\left(1-\frac{\ln\varepsilon_\vartheta}{\ln\kappa}\right)+J_c(d-2z)\varepsilon_\vartheta, \tag{2}$$

where (z,r) are the coordinates of the upper interphase surface [Fig. 1(b)]. As seen from Eq. (2), I_E decreases towards the center because of a decrease of both $(d-2z)$ and ϑ.

Variables r, z, and $\tan\vartheta=dz/dr$ are connected by equation for a cross section of the interphase surface. As noted before, the cross-section shape may in general be obtained by

solving of the Laplace equation but for anisotropic superconductor with pinning the corresponding calculations are very complicated. To avoid them, a reasonable assumption should be done about the shape. The calculated H_p may then be compared with the measured one, showing whether the chosen shape was suitable or not.

It is known that the interphase surface is convex and tangent to the sample surface at $r=R-\delta R$ due to the boundary condition for the Meissner part of a sample. In the field H_p the interphase surface gets some finite curvature at the equator. The simplest interphase surface satisfying these demands has an elliptic cross section with semiaxes δR and $d/2$ [Fig. 1(b)]. The equation for the cross section is

$$\left(\frac{R-r}{\delta R}\right)^2+\left(\frac{2z}{d}\right)^2=1. \tag{3}$$

Note, that following from Eq. (3) the equatorial curvature radius ρ of the interphase surface is equal to $\eta d/2$ where $\eta=d/2\delta R$ is a dimensionless parameter calculated below.

The applied field and the field produced by the edge current I_E should be compensated in the Meissner region $r<R-\delta R$ by the field produced by the shielding current. The latter is equal to a discontinuity of tangential component of local field at the surface of the Meissner region. A set of equations can be written for the normal and the tangential components of the field in the Meissner region that allow one to connect H_a, I_E, and I. This problem is identical to the problem of virgin magnetization in the critical state model for a thin flat superconductor when I_E is replaced by the critical current I_c. Using the known solution obtained in this model,[1,3] the following expression can be written:

$$H_a=\frac{1}{2}\int_{R-\delta R}^{R}\frac{I_E dr}{\sqrt{r^2-(R-\delta R)^2}}. \tag{4}$$

Evidently, the sheet current distribution is close to the Meissner one when $\delta R\ll R$. In the critical state model one can show that the correction for this distribution is of the order of $\delta R/R$. The Meissner current distribution coincide for a disk and an oblate spheroid with a large aspect ratio.[19] This distribution[1,15,19] $I=-(4H_a/\pi)r/\sqrt{R^2-r^2}$ is independent on sample thickness and diverges when $r\to R$ whereas the real current at the edge is limited. To understand the reason for this discrepancy a deep analogy between a superconductor in magnetic field and a conductor in electric field may be used. In particular, distribution is the same for both shielding current and surface charge density because they are calculated from the same Laplace equation.[20] As is well known from electrostatics, the latter is proportional to the local surface curvature. The same should be valid for the shielding current density. Therefore one can conclude that the local edge currents and the local edge fields coincide for a thin disk and a spheroid with equal diameters and edge curvature radii.

In field H_p the equatorial field reaches H_{c1} and the equatorial curvature radius of the Meissner part of the sample is $\rho=\eta d/2$. The same field is reached at equator of the spheroid with the same equatorial curvature radius $\rho=b^2/R=\eta d/2$ where b is minor semiaxis. The major-to-minor semiaxis ratio of such a spheroid is $c=R/b=\sqrt{a/\eta}$. The field at the equator of a spheroid is equal to applied field multiplied by enhancement factor $N=1/(1-e)$ where e is the demagnetizing factor. For an oblate spheroid one can write[21]

$$N=\frac{(c^2-1)^{3/2}}{c^2\arctan\sqrt{c^2-1}-\sqrt{c^2-1}}. \tag{5}$$

As a result, the expression for the penetration field can be written

$$H_p=\frac{H_{c1}}{N(\sqrt{a/\eta})}. \tag{6}$$

Comparing the right-hand sides of Eqs. (4) and (6), using Eqs. (2) and (3), introducing dimensionless variable $(R-r)/\delta R=y$ and parameter $h_0=J_c d/2H_{c1}$, one can finally write

$$\frac{1}{N(\sqrt{a/\eta})}=\int_0^1\frac{\varepsilon\left[1-\dfrac{\ln\varepsilon}{\ln\kappa}+h_0(1-\sqrt{1-y^2})\right]}{\sqrt{y(2a\eta-2+y)}}dy, \tag{7}$$

$$\varepsilon=\sqrt{1-(1-\gamma)(y^2-1)/[1+y^2(\eta^2-1)]}.$$

Calculating η from Eq. (7) one easily obtains both H_p and δR which can be measured experimentally.

Consider first the zero-pinning behavior. For isotropic superconductor $I_E=\text{const}$, the integral can be calculated analytically and Eq. (7) is reduced to

$$\frac{1}{N(\sqrt{a/\eta})}=\ln\left(\frac{a\eta+\sqrt{2a\eta-1}}{a\eta-1}\right). \tag{8}$$

In the limit $a\to\infty$ the value of $\eta=2\sqrt{2}/\pi$ is close to unity. Such a value agrees well with the estimate made when the GBM was developed.[22] Figure 2 shows $H_p(a)$ and $\delta R(a)$ calculated for isotropic and anisotropic ($\gamma=0.04$, $\kappa=80$) superconductor. The penetration field of isotropic superconductor decreases similar as $1/\sqrt{a}$. In the limit $a\to\infty$ the edge width tends to some constant value which increases with anisotropy growth. In Fig. 3 the dependencies of H_p and δR on anisotropy are depicted. As seen, H_p decreases and δR increases with anisotropy growth. The dependence of this parameters on κ is logarithmically weak.

The next step is to account pinning influence. The calculated $H_p(h_0)$ and $\delta R(h_0)$ for isotropic and anisotropic ($\gamma=0.04$, $\kappa=80$) superconductor are depicted in Fig. 4 which clearly demonstrates that pinning suppresses the edge width and enlarges the penetration field. Pinning influence increases under growth of both anisotropy and aspect ratio.

The model developed in this section allows one to calculate the edge width and the penetration field for any set of parameters. As an example we have numerically calculated $H_p(a,h_0)$ for $\gamma=0.04$ and $65\leqslant\kappa\leqslant80$, which are close to those values for $YBa_2Cu_3O_{7-\delta}$, and fitted the obtained dependence to the function $H_p=H_{c1}x/a^y$, where $x=0.858[1+0.643\ln(1+h_0/6.666)]$, $y=0.495[1-0.0117(h_0-0.5)]$. In the ranges $10\leqslant a\leqslant200$ and $0\leqslant h_0\leqslant10$ the fit accuracy is better than 3.5%. In the next section we compare the calculated and the measured penetration field for $YBa_2Cu_3O_{7-\delta}$

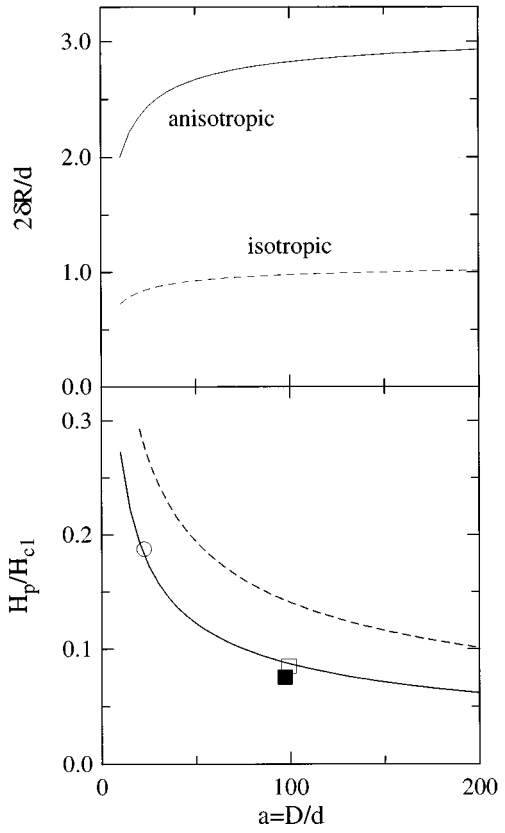

FIG. 2. H_p and δR vs aspect ratio for the pinning-free isotropic (dash) and anisotropic (solid) ($\gamma=0.04$, $\kappa=80$) superconductors. Open and closed symbols are the experimental data for $YBa_2Cu_3O_{7-\delta}$ single crystals at $T<10$ K (○: Ref. 28, □: Ref. 10) and $T=85$ K (Ref. 4), respectively. For detailed explanation, see the text.

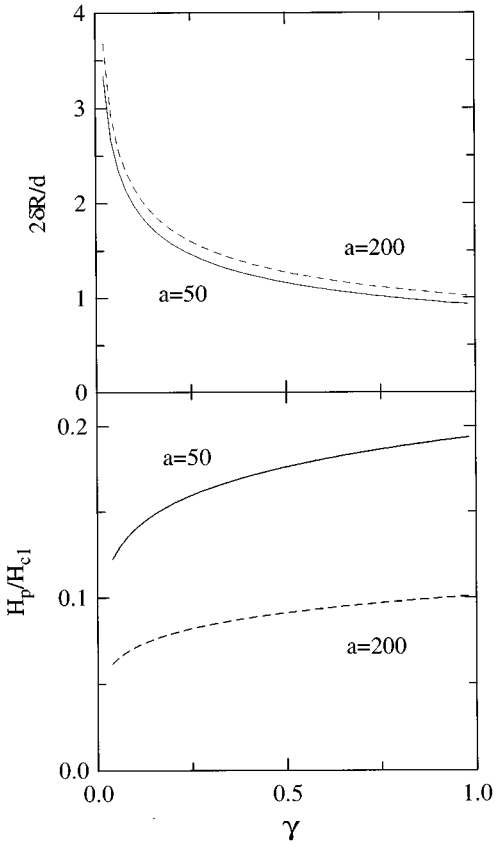

FIG. 3. H_p and δR vs anisotropy for a pinning-free superconductor. Curves were calculated when $\kappa=80$.

single crystals to test a validity of the assumption made about the shape of the cross section of the interphase surface.

III. DISCUSSION

All expressions for the penetration field contain also the lower critical field. Let us briefly discuss the lower critical field of HTSC's. Experimental data on low-temperature behavior of both H_{c1} and λ are quite different. From one hand, two-fluid or BCS-like $\lambda(T)$ dependence have been observed for all HTSC's.[23] From the other hand, precise measurements have exposed a linear increase of the penetration depth at low temperatures which is regarded as a manifestation of the d-wave pairing in HTSC's.[24] It also has been observed that defects and impurities can change dependence of $\lambda(T)$ from a linear into a quadratic one.[24,25] In addition to that mentioned above, in layered HTSC's λ is affected by dynamics of pancake vortices which strongly depends on temperature.[26,27] Summing up, one can conclude that $\lambda(T)$ behavior depends on the type of HTSC's and perfection of its crystalline structure. This conclusion is confirmed by measurements of the lower critical field. Saturation of $H_{c1}(T)$,[10,28] as well as linear decrease with T, have been observed.[27,29]

It should be noted that in the present work we do not consider the pancake vortices attributed to the layered superconductors. Angular dependence of the lower critical field in these superconductors[30] differs from expression (1) used in our calculations. Therefore the layered Bi or Tl-based HTSC's characterized by a weak pinning are unlikely useful to test the model. Pinning is strong enough to affect the temperature dependence of the penetration field of other HTSC's.

A. Temperature dependence of the penetration field

In the pinning-free case η and δR are independent of temperature. Therefore H_p and the lower critical field have the same temperature dependence. When pinning is present, the temperature dependence of the lower critical field can be derived from that of the penetration field and the critical current, which may be measured directly.[31] To do this, one should combine Eqs. (6) and (7) in the unknown η and H_{c1} at any temperature, using measured $J_c(T)$ and $H_p(T)$ as parameters.

Let us consider influence of pinning on the penetration field of HTSC's single crystals. The value of h_0 in Eq. (7) depends on both H_{c1} and J_c. For simplicity, neglecting slight temperature dependence of $\ln(\kappa)$, we use expression $H_{c1}(T)=H_{c1}(0)(1-t^4)$ from the two-fluid model where $t=T/T_c$ and T_c is the critical temperature. $J_c(T)$ of HTSC's single crystals can be well described by the following empirical dependence:[32]

$$J_c(T)=J_c(0)[\exp(-T/T_0)-\exp(-T_c/T_0)], \qquad (9)$$

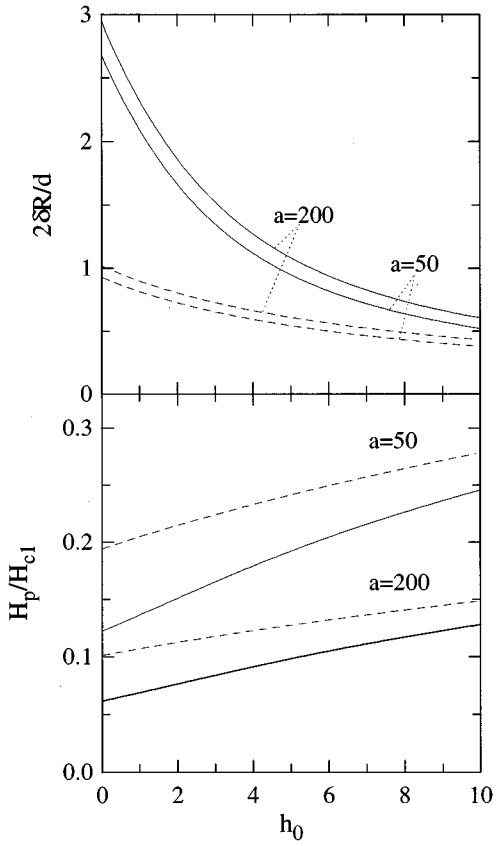

FIG. 4. H_p and δR vs parameter h_0 for isotropic (dash) and anisotropic (solid) ($\gamma=0.04$, $\kappa=80$) superconductor.

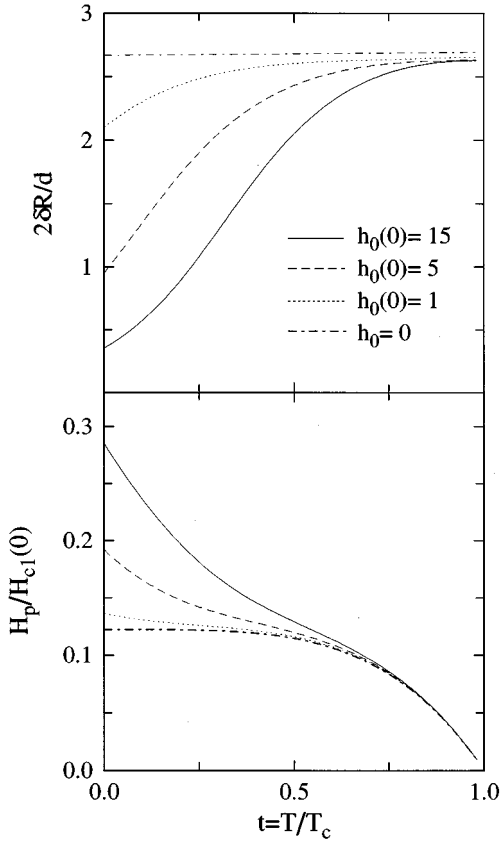

FIG. 5. Temperature dependences of H_p and δR. The calculations were made for $a=50$, $\gamma=0.04$, $\kappa=80$, and $T_c/T_0=5$.

where the characteristic temperature T_0 varies in the range from 10 K to 30 K depending on type of superconductor.

The curves $H_p(t)$ and $\delta R(t)$ calculated for the sample with $a=50$, $\gamma=0.04$, $\kappa=80$, and $T_c/T_0=5$ are plotted in Fig. 5. As seen, pinning results in the absence of low-temperature saturation of H_p and the increase of δR with temperature.

We used $H_{c1}(T)$ dependence which saturates at low temperature. Critical current decreases with T at this range. If H_{c1} also decreases, the ratio $h_0(T)$ is larger than in the previous case. As seen from Fig. 5 the larger h_0 the stronger pinning influence.

For typical HTSC's single crystals with $d\simeq 50$–100 μm, $J_c(0)\simeq 5\times 10^9$ A m^{-2}, and $\mu_0 H_{c1}(0)=20$–40 mT, the value of $h_0(0)\simeq 4$–16 is rather large. It grows with the thickness of a sample but is independent of the transverse size. We conclude that pinning strongly affects $H_p(T)$ of such crystals at low temperatures.

B. Penetration field of $YBa_2Cu_3O_{7-\delta}$ single crystals

We can now compare the calculated $H_p(a)$ with the available data. We have chosen $YBa_2Cu_3O_{7-\delta}$ which is currently the most investigated HTSC's with $\gamma\simeq 0.04$, penetration depth $\lambda_{ab}(0)=140$ nm,[23] and correlation length $\xi_{ab}(0)=1.72$ nm,[33] which give $\mu_0 H_{c1}(0)=41.3$ mT. To diminish the influence of pinning the experimental results obtained for very thin samples, $d=4$ μm (Refs. 4,10,34) and $d=10$ μm,[28] were selected. The estimated value of h_0 does not exceed 0.3 for the thinner sample and has smaller value for the thicker one because the measurements performed for the latter in Ref. 28 were carried out at high frequency when J_c is strongly suppressed. We estimated that the correction to H_p due to pinning does not exceed 6% for these samples, so we compare the measured penetration field with $H_p(a)$ calculated for the pinning-free case. The aspect ratios, $a=97$,[4] $a=99$,[10] and $a=22.6$,[28] were calculated in a way given in Ref. 35. The penetration field values, $\mu_0 H_p=0.52$ mT at $T=85$ K,[4] $\mu_0 H_p=3.5$ mT at $T=5$ K,[10] and $\mu_0 H_p=7.73$ mT at $T=10$ K,[28] were normalized to the corresponding values of $H_{c1}(t)$.[36]

As seen from Fig. 2, the values measured at low temperature (open symbols) demonstrate a good agreement with the calculated values of $H_p(a)$, whereas the value measured at high temperature (closed symbol) deviates from the calculated one. We suppose that the deviation is caused by a small thickness of the sample which makes our model invalid, as shown below.

C. Limitations on sample parameters

Consider limitations on sample parameters following from the assumptions made above.

To describe the edge current the expression (2) was used. We assumed that the current flowing at the interphase surface is equal to a sum of shielding currents at top and bottom

parts of the surface. If the distance between the opposite parts is comparable with the decay length of the shielding current, this expression fails because shielding currents are overlapped. The minimal distance is of the order of the equatorial curvature radius $\rho = d\eta/2$. The decay length is less than or of the order of $\lambda/\sqrt{\gamma}$, where λ is the penetration depth for the isotropic plane. We conclude that the presented description of the edge effects is valid only for samples which are thicker than $d_c \simeq 2\lambda/(\eta\sqrt{\gamma})$. For a single crystal of $YBa_2Cu_3O_{7-\delta}$ with $a \simeq 100$ one has $d_c \simeq 4$ μm at low temperature, and $d_c \simeq 10$ μm at 85 K. The latter value exceeds the thickness of the sample investigated in Ref. 4. Therefore the calculated H_p is invalid in this case.

To obtain expression (6) the sample was approximated by an oblate spheroid with $b \ll R$. Because the value of $\sqrt{\eta}$ is of the order of unity, this condition, which can be rewritten as $\sqrt{a} \gg \sqrt{\eta}$, is stronger than the general requirement $a \gg 1$ for a thin flat sample.

Apparently, the developed model cannot be applied to thin films with $d < \lambda$. The virgin flux penetration into films is well described by the critical state model[1–3] in which the value of the penetration field is assumed to be negligibly small. When pinning is strong, this assumption is valid. In the case of weak pinning a transition to the mixed state can be impeded by the Bean-Livingston barrier arising from the finite energy of a vortex nucleation at the film edge.[37] The problem of a vortex located near the edge of a film has been recently solved by Kogan.[38] The obtained dependencies of the energy and the magnetic moment of the vortex on a distance from the edge allow one to estimate the penetration field of a film.

IV. SUMMARY

In this paper we have considered the onset of flux penetration into a type-II superconductor with rectangular cross section. The results obtained show that anisotropy and pinning have strong influence on the penetration field value and its temperature dependence. For disks with a large aspect ratio we have calculated the penetration field and the width of the mixed-state region at the sample edge which can be measured experimentally. We would like to note that the same quantities can be calculated for samples with arbitrary aspect ratio using a method developed by Brandt,[14] but this method should be extended to both anisotropic and pinning-free cases.

In conclusion we point out the following main results obtained in the present work.

(1) A simple model has been developed to calculate the penetration field of the geometrical barrier taking into account anisotropy and pinning.

(2) It has been found that the published experimental data on the penetration field of platelike $YBa_2Cu_3O_{7-\delta}$ single crystals agree with the calculated values of H_p.

(3) It has been shown that pinning of vortices in the corners of a sample strongly affects $H_p(T)$ of platelike HTSC's single crystals at low temperatures.

ACKNOWLEDGMENTS

The authors are indebted to Professor V. A. Kashurnikov, Dr. A. A. Sinchenko, Dr. A. A. Ivanov, and K. V. Klementev for helpful discussions. We are grateful to Professor A. P. Menushenkov for his support of the present investigation.

[1] P. N. Mikheenko and Yu. E. Kuzovlev, Physica C **204**, 229 (1993); J. Zhu, J. Mester, J. Lockhart, and J. Turneaure, *ibid.* **212**, 216 (1993); John R. Clem and Alvaro Sanchez, Phys. Rev. B **50**, 9355 (1994); A. V. Kuznetsov, A. A. Ivanov, D. V. Eremenko, and V. Trofimov, *ibid.* **52**, 9637 (1995).

[2] E. H. Brandt, M. Indenbom, and A. Forkl, Europhys. Lett. **22**, 735 (1993); E. H. Brandt and M. Indenbom, Phys. Rev. B **48**, 12 893 (1993); E. H. Brandt, *ibid.* **49**, 9024 (1994); **50**, 4034 (1994); A. Gurevich and E. H. Brandt, Phys. Rev. Lett. **73**, 178 (1994); E. Zeldov, John R. Clem, M. McElfresh, and M. Darwin, Phys. Rev. B **49**, 9802 (1994).

[3] J. McDonald and John R. Clem, Phys. Rev. B **53**, 8643 (1996).

[4] M. Konczykowski, L. I. Burlachkov, Y. Yeshurun, and F. Holtzberg, Phys. Rev. B **43**, 13 707 (1991).

[5] N. Chikumoto, M. Konczykowski, N. Motohira, and K. Kishio, Physica C **199**, 32 (1992); M. Xu, D. K. Finnemore, G. W. Crabtree, V. M. Vinokur, B. Dabrowski, D. G. Hinks, and K. Zhang, Phys. Rev. B **48**, 10 630 (1993); D. Majer, E. Zeldov, and M. Konczykowski, Phys. Rev. Lett. **75**, 1166 (1995).

[6] M. V. Indenbom, H. Kronmüller, T. W. Li, P. H. Kes, and A. A. Menovsky, Physica C **222**, 203 (1994).

[7] E. Zeldov, A. I. Larkin, V. B. Geshkenbein, M. Konczykowski, D. Majer, B. Khaykovich, V. M. Vinokur, and H. Shtrikman, Phys. Rev. Lett. **73**, 1428 (1994); E. Zeldov, A. I. Larkin, M. Konzykowski, B. Khaykovich, D. Majer, V. B. Geshkenbein, and V. M. Vinokur, Physica C **235-240**, 2761 (1994).

[8] C. P. Bean and J. D. Livingston, Phys. Rev. Lett. **12**, 14 (1964); V. P. Galaiko, Zh. Éksp. Teor. Fiz. **50**, 1322 (1966) [Sov. Phys. JETP **23**, 878 (1966)]; John R. Clem, in *Proceedings of the 13th Conference on Low Temperature Physics* (LT 13), edited by K. D. Timmerhaus, W. J. O'Sullivan, and E. F. Hammel (Plenum, New York, 1974), Vol. 3, p. 102; B. V. Petukhov and V. R. Chechetkin, Zh. Éksp. Teor. Fiz. **65**, 1653 (1973) [Sov. Phys. JETP **38**, 827 (1974)].

[9] V. N. Kopylov, A. E. Koshelev, I. F. Schegolev, and T. G. Togonidze, Physica C **170**, 291 (1990); L. Burlachkov, Phys. Rev. B **47**, 8056 (1993); L. Burlachkov, V. B. Geshkenbein, A. E. Koshelev, A. I. Larkin, and V. M. Vinokur, *ibid.* **50**, 16 770 (1994).

[10] L. Burlachkov, Y. Yeshurun, M. Konczykowski, and F. Holzberg, Phys. Rev. B **45**, 8193 (1992).

[11] J. Provost, E. Paumier, and A. Fortini, J. Phys. F **4**, 439 (1974); A. Fortini, E. Paumier, J. Provost, and J.-P. Girard, J. Phys. (Paris) Suppl. **8**, 427 (1973) (in French); A. Fortini and E. Paumier, Phys. Rev. B **14**, 55 (1976); A. Fortini, A. Hairie, and E. Paumier, *ibid.* **21**, 5065 (1980); A. Fortini, A. Hairie, and J.-P. Girard, J. Math. Phys. (N.Y.) **20**, 2139 (1979).

[12] M. Benkraouda and J. R. Clem, Phys. Rev. B **53**, 5716 (1996).

[13] I. L. Maksimov and A. A. Elistratov, Pis'ma Zh. Éksp. Teor. Fiz. **61**, 204 (1995) [Sov. JETP Lett. **61**, 208 (1995)].

[14] E. H. Brandt, Phys. Rev. B **54**, 4246 (1996).

[15] V. N. Trofimov, A. V. Kuznetsov, P. V. Lepeshkin, K. A.

Bolshinskov, A. A. Ivanov, and A. A. Mikhailov, Physica C **183**, 135 (1991); V. N. Trofimov and A. V. Kuznetsov, *ibid.* **235-240**, 2853 (1994).

[16] R. Olafsson and J. R. Allen, J. Phys. F **2**, 123 (1972).

[17] R. Klemm and J. R. Clem, Phys. Rev. B **21**, 1868 (1980).

[18] G. Blatter, M. V. Feigel'man, V. B. Geshkenbein, A. I. Larkin, and V. M. Vinokur, Rev. Mod. Phys. **66**, 1125 (1994).

[19] M. B. Ketchen, W. J. Gallagher, A. W. Kleinsasser, S. Murphy, and J. R. Clem, in *SQUID'85-Superconducting Quantum Interference Devices and Their Applications*, edited by H. D. Hahlbohm and H.Lübbig (Walter de Gruyter & Co., Berlin, 1985), p. 865.

[20] L. D. Landau and E. M. Lifshits, *Electrodynamics of Continuous Media* (Pergamon, London, 1982), VI. 55.

[21] In Ref. 15 the Laplace equation has been solved in a limit of small eccentricity $\epsilon = 1/a \to 0$. The scalar potential Ψ of magnetic field for arbitrary a is $\Psi = -H_a c\sigma\tau(1 + A[\arctan(1/\sigma) - 1/\sigma)]$, where $A = a^2/(\sqrt{a^2-1} - a^2 \arctan\sqrt{a^2-1})$, c is an interfocus length, and other notations are defined in Ref. 15. Equation (5) for enhancement factor of a spheroid $N = (H_\tau/H_a)|_{\tau\to 0}$, which relates a tangential component of the equatorial field H_τ to the applied one, is obtained for the general solution of the Laplace equation.

[22] In Ref. 7 it is assumed that vortices penetrate initially into the edge rim of width $\delta R \simeq d/2$. In Ref. 12 a flat sample with rounded edge and equatorial curvature radius $\rho = d/2$ is considered. The corresponding calculated values are $\delta R \simeq \pi d/4\sqrt{2}$ and $\rho \simeq \sqrt{2} d/\pi$.

[23] Quiang Li, M. Suenaga, T. Kimura, and K. Kishio, Phys. Rev. B **47**, 2854 (1993) [$(La_{1-x}Sr_x)_2CuO_4$]; A. Adreone, A. Gassinese, A. Di Chiara, R. Vaglio, A. Gupta, and E. Sarnelli, *ibid.* **49**, 6392 (1994) [$Nd_{1.85}Ce_{0.15}CuO_{4-\delta}$); A. Schilling, F. Hulliger, and H. R. Ott, Physica C **168**, 272 (1990); P. Zimmermann, H. Keller, S. L. Lee, I. M. Savić, M. Warden, and D. Zech, R. Cubitt, E. M. Forgan, E. Kaldis, J. Karpinski, and C. Krüger, Phys. Rev. B **52**, 541 (1995) ($YBa_2Cu_3O_{7-\delta}$); P. Puźniak, R. Usami, K. Isawa, and H. Yamauchi, *ibid.* **52**, 3756 (1995) ($HgBa_2Ca_{n-1}Cu_nO_y$); B. Ravkin, T. A. Mahl, A. S. Bhalla, Z. Z. Sheng, and N. S. Dalal, *ibid.* **41**, 769 (1990) ($Tl_2Ba_2Ca_2Cu_3O_x$ and $Bi_2Sr_2CaCu_2O_x$).

[24] W. N. Hardy, D. A. Bonn, D. C. Morgan, Ruixing Liang, and Kuan Zhang, Phys. Rev. Lett. **70**, 3999 (1993); D. A. Bonn, S. Kamal, Kuan Zhang, Ruixing Liang, D. J. Baar, E. Klein, and W. N. Hardy, Phys. Rev. B **50**, 4051 (1994).

[25] J. Y. Lee, K. M. Paget, T. Lemberger, S. R. Foltyn, and X. Wu, Phys. Rev. B **50**, 3337 (1994); E. R. Ulm, J.-T. Kim, T. Lemberger, S. R. Foltyn, and X. Wu, *ibid.* **51**, 9193 (1995).

[26] D. R. Harshman, R. N. Kleinman, M. Inui, G. P. Espinosa, D. B. Mitzi, A. Kapitulnik, T. Pfiz, and D. L. Williams, Phys. Rev. Lett. **67**, 3152 (1991).

[27] A. Maeda, T. Shibauchi, N. Kondo, K. Uchinokura, and M. Kobayashi, Phys. Rev. B **46**, 14 234 (1992).

[28] Dong-Ho Wu and S. Sridhar, Phys. Rev. Lett. **65**, 2074 (1990).

[29] Ruixing Liang, P. Dosanjh, D. A. Bonn, W. N. Hardy, and A. J. Berlinsky, Phys. Rev. B **50**, 4212 (1994).

[30] J. R. Clem, Phys. Rev. B **43**, 7837 (1991). See also appropriate parts in Ref. 18.

[31] M. W. McElfresh, Y. Yeshurun, A. P. Malozemoff, and F. Holtzberg, Physica A **168**, 308 (1990); V. V. Moshchalkov, A. A. Zhukov, D. K. Petrov, V. I. Voronkova, and V. K. Yanovskii, Physica C **166**, 185 (1990); V. V. Moshchalkov, J. Y. Henry, C. Marin, J. Rossat-Mignod, and J. F. Jacquot, *ibid.* **175**, 407 (1991); L. Fàbrega, J. Fontcuberta, B. Martínez, and S. Piñol, Phys. Rev. B **50**, 3256 (1994).

[32] A. A. Zhukov and V. V. Moshchalkov, Sverhprov. Fiz. Him. Tehn. **4**, 850 (1991) [Sov. Supercond. Phys. Chem. Tech. **4**, 759 (1991)].

[33] Z. Hao, J. R. Clem, M. W. McElfresh, L. Civale, A. P. Malozemoff, and F. Holtzberg, Phys. Rev. B **43**, 2844 (1991).

[34] The sample measured in Ref. 4 was a piece of the same single crystal as in Ref. 10.

[35] For the samples differing in shape from a disk, the effective aspect ratio a was determined in a following way. A square with the aspect ratio $c \gg 1$ may be replaced by an effective disk of the same area, which has $a = 2c/\sqrt{\pi}$. An infinite strip with the width over thickness ratio $c \gg 1$ may be replaced by an elliptic cylinder. The ratio of the demagnetizing factor of the latter (Ref. 12) to that of spheroid (5) with equal cross section, gives $a = 2c/\pi$. For a rectangular plate with sides ratio l, linear extrapolation between the square and the infinite strip gives $a = (2c/\pi) \times [1 + (\sqrt{\pi} - 1)/l]$.

[36] Since saturated $H_p(T)$ dependences were observed in Refs. 10 and 28, the data obtained at $T \leqslant 10$ K were normalized to $H_{c1}(0)$. At high temperature we omitted slight dependence $\ln\kappa(t)$ and considered $H_{c1}(t)/H_{c1}(0) = H_c(t)\kappa(0)/[H_c(0)\kappa(t)]$. BCS ratio $H_c(t)/H_c(0)$ was used (Ref. 33). We fitted $\kappa(t)$ in a clean limit [G. Eilenberger, Phys. Rev. **153**, 584 (1967)] to $\kappa(t) = \kappa(0)(1 - 0.206t)$.

[37] K. K. Likharev, Izv. Vuzov ser. Radiofiz. **14**, 909 (1971); **14**, 919 (1971) (in Russian).

[38] V. G. Kogan, Phys. Rev. B **49**, 15 874 (1994).